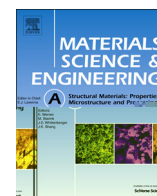




ELSEVIER

Contents lists available at SciVerse ScienceDirect

Materials Science & Engineering A

journal homepage: www.elsevier.com/locate/msea

Rapid communication

Room-temperature anelasticity and viscoplasticity of Cu–Zr bulk metallic glasses evaluated using nanoindentation

Byung-Gil Yoo^{a,b}, In-Chul Choi^a, Yong-Jae Kim^a, Upadrasta Ramamurty^c, Jae-il Jang^{a,*}^a Division of Materials Science and Engineering, Hanyang University, Seoul 133-791, Republic of Korea^b Institute for Applied Materials, Karlsruhe Institute of Technology, Karlsruhe 76131, Germany^c Department of Materials Engineering, Indian Institute of Science, Bangalore 560012, India

ARTICLE INFO

Article history:

Received 26 February 2013

Accepted 10 April 2013

Available online 17 April 2013

Keywords:

Bulk metallic glass

Nanoindentation

Anelasticity

Viscoplasticity

ABSTRACT

Anelastic and viscoplastic characteristics of Cu₅₀Zr₅₀ and Cu₆₅Zr₃₅ binary bulk metallic glasses at room temperature were examined through nanoindentation creep experiments. Results show that both the deformations are relatively more pronounced in Cu₅₀Zr₅₀ than in Cu₆₅Zr₃₅, and their amount increases with the loading rate. The results are analyzed in terms of the influences of structural defects and loading rate on the room temperature indentation creep.

© 2013 Elsevier B.V. All rights reserved.

1. Introduction

The elastic and plastic responses of metallic glasses are fundamentally different from those of the crystalline materials. With the recent discovery of bulk metallic glasses (BMGs), there has been considerable interest in understanding their mechanical behavior [1,2]. Of late, the time-dependent deformation behavior of these amorphous alloys is also getting much attention [3–5]. The nanoindentation technique is particularly useful for studying such behavior for two important reasons: First, the available size of good quality BMG samples is still limited. Since nanoindentation needs only small volume of the testing material, it can be utilized extensively for the assessment of the time-dependent properties in BMGs (see for example, our recent work on this aspect [6–8]). Second, BMGs exhibit negligible tensile plasticity—due to localization of flow into shear bands and unmitigated propagation of them. While the behavior in uniaxial compression is slightly better, issues like buckling and barreling in addition to flow initiation at specimen corners complicate the matter. In this context, indentation is advantageous as it imparts intrinsically stable deformation behavior to the material underneath the indenter. As a result, it has been widely used to study the plastic deformation behavior of BMGs [9–11].

Typically, materials are expected to creep at high homologs temperatures (T/T_m where T is the testing temperature and T_m is the melting temperature of the material that is being examined).

However, prior nanoindentation experiments showed that the creep can occur even at room temperature not only in the BMGs with low glass transition temperature, T_g (and thus high reduced temperature, T/T_g , of 0.7–0.75 as in the case of Ce- and Mg-based BMGs [12,13]) but also in BMGs with high T_g (with T/T_g 0.3–0.4 as in Ti- and Fe-based BMGs [14,15]).

Just as the deformation behavior of material can be partitioned into elastic and plastic components, the time-dependent deformation can also be separated into anelastic and viscoplastic parts, which correspond to recoverable and permanent parts, respectively. (Aside, it has been also reported that some portion of the creep strain in metallic glasses can be recovered when the applied stress is removed [16,17].) However, a systematic analysis as to how the time-dependent deformation of metallic glasses partitions into these has not been conducted yet. To this end, we examine the room temperature anelasticity and viscoplasticity during nanoindentation creep of Cu₅₀Zr₅₀ and Cu₆₅Zr₃₅ BMGs, which are known to be distinctly different in terms of the as-cast free volume content in them. While Cu₅₀Zr₅₀ has perhaps the largest amount of free volume amongst various bulk-forming Cu–Zr amorphous alloys, Cu₆₅Zr₃₅ has arguably the lowest [18]. This difference is the as-cast structural state of the alloy also gets reflected in their plastic deformation responses; while Cu₅₀Zr₅₀ is ductile and Cu₆₅Zr₃₅ is brittle [18]. This is illustrated in Fig. 1, wherein the compressive stress–strain responses obtained on these two alloy samples are displayed. Thus, by comparing the nanoindentation responses of these two glasses, we also examine the influence of intrinsic structural state of the glass as well as the loading rate, dP/dt , on the time-dependent deformation characteristics of BMGs.

* Corresponding author. Tel.: +82 2 2220 0402; fax: +82 2 2220 0389.
E-mail address: jjjang@hanyang.ac.kr (J.-i. Jang).

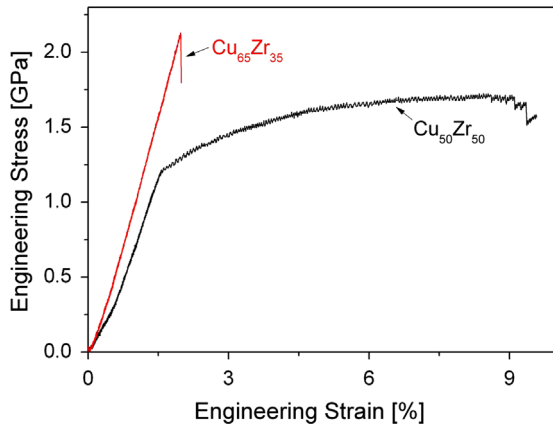


Fig. 1. Compressive stress–strain curves of the $\text{Cu}_{50}\text{Zr}_{50}$ and $\text{Cu}_{65}\text{Zr}_{35}$ samples.

2. Experimental

Two 1 mm diameter rods of Cu–Zr binary amorphous alloys, $\text{Cu}_{50}\text{Zr}_{50}$ and $\text{Cu}_{65}\text{Zr}_{35}$, were prepared by Cu mold casting. The amorphous nature of the cast samples was ascertained through X-ray diffraction. Nanoindentation experiments were performed using a Nanoindenter-XP (former MTS; now Agilent, Oak Ridge, TN) equipped with a Berkovich tip. During the test, the load was increased up to peak load, P_{max} , of 50 mN at different dP/dt of 0.1, 0.5, and 2.5 mN/s. In all cases, the sample was held at P_{max} for 400 s so as to measure the time-dependent displacement. Subsequently, the samples were unloaded to 0.5 mN (all at a fixed rate of 2.5 mN/s) and held again for 400 s, so as to measure the time-dependent recovery of the deformation. The profiles of the indented surfaces were examined by atomic force microscopy (AFM) XE-100 (Park Systems, Suwon, Korea).

3. Results

Fig. 2(a) compares the representative load–displacement (P – h) responses of $\text{Cu}_{50}\text{Zr}_{50}$ and $\text{Cu}_{65}\text{Zr}_{35}$, obtained at $dP/dt=2.5$ mN/s. It shows that $\text{Cu}_{50}\text{Zr}_{50}$ exhibits (a) significantly larger displacement during loading and (b) more pronounced time-dependent deformation (i.e., an increase in h during the hold period at P_{max}) than $\text{Cu}_{65}\text{Zr}_{35}$. This suggests that $\text{Cu}_{65}\text{Zr}_{35}$ is not only more resistant to plastic deformation during quasi-static loading, as already seen through the uniaxial compression tests, but also offers a higher resistance to time-dependent deformation. Fig. 2(b) summarizes the variation in the total creep displacement at hold, h_c , with dP/dt . The inset figure shows time–displacement curves during the hold period for the $\text{Cu}_{50}\text{Zr}_{50}$ alloy. While h_c in $\text{Cu}_{65}\text{Zr}_{35}$ is negligible and rate-independent, h_c in $\text{Cu}_{50}\text{Zr}_{50}$ is significant and increases markedly with dP/dt .

Since h_c is a sum of the anelastic and the viscoplastic deformation, the relative contribution of anelasticity can be estimated from the recovered displacement during hold period of the unloading sequence. Note that here we adopted a sharp indenter, although spherical indentation or micro-pillar compression are likely to produce conditions that are more akin to those experienced in a conventional uniaxial creep test [6,8,19]. In spite of this, the anelastic portion of the total creep deformation obtained with a sharp tip can be considered to be similar to the recovery amount because the stress state underneath a sharp tip remains affine during entire loading and unloading sequences, in contrast to that of the spherical indentation.

Variation in the total displacement recovery during hold at 0.5 mN, h_r , with dP/dt is shown in Fig. 3(a). Again, the $\text{Cu}_{50}\text{Zr}_{50}$ sample exhibits relatively large h_r and is rate-dependent, whereas

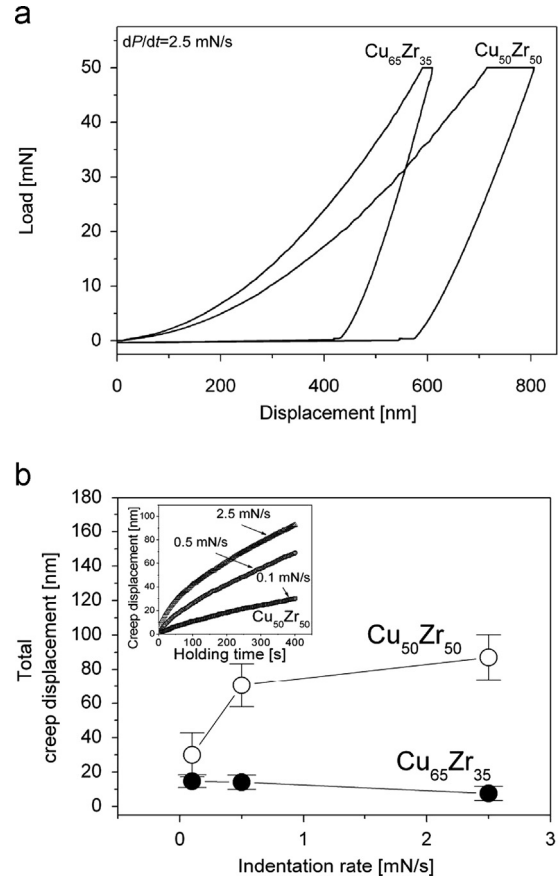


Fig. 2. Creep behavior of the $\text{Cu}_{50}\text{Zr}_{50}$ and $\text{Cu}_{65}\text{Zr}_{35}$ samples (a) representative load–displacement curves (obtained at $dP/dt=2.5$ mN/s) and (b) variation in total creep displacement with loading rate. The inset shows displacement vs. time plot obtained during load-holding sequence.

recovery of the $\text{Cu}_{65}\text{Zr}_{35}$ sample is almost negligible. The inset of Fig. 3(a) shows the variation in displacement recovery ($=h_0-h$, where h_0 is the displacement at the start of the hold during unloading) against t . Assuming that the recovery that occurs during this hold is entirely anelastic, these plots can be converted into anelastic time–displacement curves as shown in the inset of Fig. 3(b). These, then, can be expressed as a sum of exponential decays based on the Kelvin model [17],

$$h = \sum_{i=1}^n h_i \left(1 - \exp\left(-\frac{t}{\tau_i}\right) \right) \quad (1)$$

where t is the holding time, h_i and τ_i are the indentation depth and the characteristic relaxation time, respectively, for the i th anelastic Kelvin element. An excellent fit ($R^2 \geq 0.99$) of Eq. (1), with a sum of only two exponential decays, to the recovery curves in the inset of Fig. 3(b) was obtained. The values of the fitting parameters are listed in Table 1. It is noteworthy that this fitting is much simpler than that for polymers, implying the anelastic deformation of BMGs is simpler, as reported before [12]. While τ_i shows no clear rate dependency, h_i increases with loading rate, which is in agreement with a prior study of Concustell et al. [20].

It has been suggested that anelasticity during indentation of metallic glasses can be analyzed in terms of a spectrum of the characteristic relaxation times τ [21], with the spectrum represented as [12,13]

$$L(\tau) = \left[\sum_{i=1}^n \left(1 + \frac{t}{\tau_i} \right) \frac{h_i}{\tau_i} \exp\left(-\frac{t}{\tau_i}\right) \right] \frac{t}{H_0 h_{in}} \Big|_{t=2\tau} \quad (2)$$

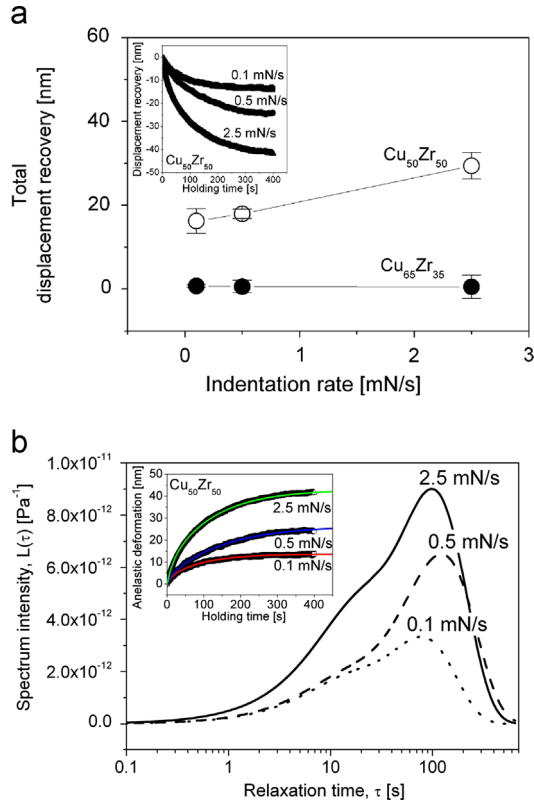


Fig. 3. Analysis of anelastic deformation; (a) results of total recovery displacement (with the inset showing displacement recovery during load-holding sequence); (b) relaxation time spectra of the Cu₅₀Zr₅₀ sample from the anelastic curve in the inset.

Table 1

Parameters from the fits of the recovery curve in the inset of Fig. 3(b) using Eq. (1).

dP/dt [mN/s]	h_1	τ_1	h_2	τ_2	R^2
0.1	10.96	95.22	2.80	13.10	0.99
0.5	23.63	150.93	2.90	12.04	0.99
2.5	34.55	121.51	8.34	15.70	0.99

where H_0 is the hardness and h_{in} is the maximum indentation depth. Fig. 3(b) shows the relaxation time spectra of the Cu₅₀Zr₅₀ sample. It is seen that each spectrum consists of two relatively separated peaks, one at around ~10 s and the other at ~100 s. This implies two kinds of relaxation processes in this BMG, which, in principle, should correlate with two different types of defects depending on chemical and topological short-range orders [12]. Through positron annihilation spectroscopy (PAS) analysis, Castellero et al. [13] suggested that the short and long lifetime peaks (i.e., activation of two distinct processes) may be attributed by small defects (intrinsic open volume region) and large (and thermally unstable) defects, respectively; the anelastic deformation tends to occur first in the volume elements for a lower degree of local relaxation (i.e., small defects) because the lower activation energy is required for the reversible transition from one energy configuration to another [13]. In Fig. 3(b), an increase in the peak intensity with dP/dt is also noted, which indicates that the increase in dP/dt leads to higher population of structural defects. We will return to this later.

The difference between the absolute values of h_c and h_r , $h_f (=h_c - h_r)$ gives the amount of visco-plastic deformation that has occurred due to hold at 50 mN. Fig. 4(a) shows the variation in h_f with dP/dt . It is noteworthy that significant levels of h_f remain in

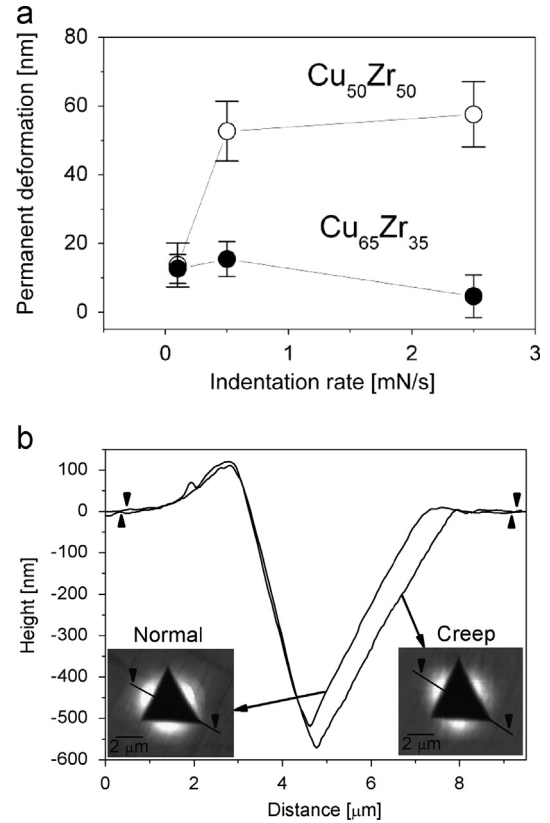


Fig. 4. Analysis of viscoplastic deformation; (a) variation in permanent deformation with loading rate; (b) representative morphologies obtained from AFM analysis.

Cu₅₀Zr₅₀ alloy, at $dP/dt=0.5$ and 2.5 mN/s. The AFM profiles of the nanoindentation impressions of the normal indented sample (i.e. without any hold period at P_{max}) and creep tested samples are shown in Fig. 4(b). From the representative line-scan profiles made across the indents, it is obvious that the final indentation depth for the crept sample is higher than that for the normal one while the material pile-up around the indentation is similar.

4. Discussion

The above results convincingly show that (a) the Cu₅₀Zr₅₀ BMG (with $T_g \sim 693$ K) indeed creeps at room temperature ($\sim 0.43T_g$) and (b) the initial structural state of the BMG markedly affects its time-dependent deformation behavior. We invoke the shear transformation zones (STZs) model [1,22], widely utilized to describe the physics of plastic deformation in amorphous materials, to rationalize these. Note that this model is applicable irrespective of the macroscopic deformation mode (i.e., instantaneous or time-dependent; homogeneous or inhomogeneous). Typically, the operation of STZs is aided by the free volume in the material, i.e. STZs preferentially get activated in those regions where the free volume content is high. Thus, a higher initial free volume content results in easier and more profuse activation of STZs, which in turn leads to higher plasticity. Therefore, a BMG with higher initial free volume would exhibit lower resistance to any mode of deformation. The observed anelasticity in Cu₅₀Zr₅₀ can also be explained on the same basis, as the free volume enhances the probability of local topology becoming unstable, which in turn results in the anelastic reshuffling of atomic near-neighbors [1]. Although only a small number of atoms may be involved in the anelastic behavior of the glass, the local strains

are large enough that their cumulative effect makes a significant contribution to the macroscopic strain [1].

The results also show that in $\text{Cu}_{50}\text{Zr}_{50}$ higher dP/dt leads to larger levels of both anelastic and viscoplastic deformations. At first sight, this appears to be somewhat of a contradictory result, as displacements associated with these deformations were measured during the hold period, i.e. P is held constant. Thus, the prior loading rate should, in principle, not matter. A possible explanation for the observed rate-dependency can be offered from earlier studies wherein it has been observed that faster rate of loading induces a higher energy state [1,22,23]. For instance, de Hey et al. [24] showed that faster loading leads to a higher production rate of excess free volume (and thus more STZs). Note that, at steady state, plasticity in metallic glasses is a balance between free volume creation and annihilation [23]. However, as dP/dt increases, more free volume is created in the material, which aids in visco-plastic deformation during the hold period. This hypothesis is supported by the clear increase in the spectrum peak intensity with dP/dt in Fig. 3(b). In addition, at higher loading rate, some portion of the plastic flow (for which there is not sufficient time during the loading) could have been delayed. Such delayed deformation can accrue during the holding sequence, which is similar to the observation by Concustell et al. [25]. For $\text{Cu}_{65}\text{Zr}_{35}$, the rate dependency of viscoplasticity is unclear since the amount of permanent deformation for each rate is too small and its standard deviation is relatively large. Further detailed examination on a variety of metallic glasses, with different initial free volume contents, may give more insights into these dynamics of anelastic and viscoplastic deformations in metallic glasses.

5. Conclusions

In summary, we have investigated the room temperature anelasticity and viscoplasticity of the $\text{Cu}_{50}\text{Zr}_{50}$ and $\text{Cu}_{65}\text{Zr}_{35}$ amorphous alloys by performing nanoindentation creep experiments under three different loading rates. Our results reveal that the glass with higher free volume content is susceptible to both anelastic and viscoplastic deformations. The time-dependent deformation characteristics in BMGs is strongly affected by both internal material condition (initial structural defects) and external testing conditions (loading rate).

Acknowledgments

This research was supported by Basic Science Research Program through the National Research Foundation of Korea (NRF) funded by the Ministry of Education, Science and Technology (No. 2010-0025526), and partly by the Human Resources Development of Korea Institute of Energy Technology Evaluation and Planning (KETEP) grant funded by the Korea government Ministry of Knowledge Economy (No. 20114010203020). The authors thank Ms. Kyoung-Won Park at KIST for providing the BMG samples examined in this work.

References

- [1] C.A. Schuh, T.C. Hufnagel, U. Ramamurty, *Acta Mater.* 55 (2007) 4067–4109.
- [2] A.R. Yavari, J.J. Lewandowski, J. Eckert, *MRS Bull.* 32 (2007) 635–638.
- [3] K.-W. Park, C.-M. Lee, M. Wakeda, Y. Shibutani, M.L. Falk, J.-C. Lee, *Acta Mater.* 56 (2008) 5440–5450.
- [4] S.-J. Lee, B.-G. Yoo, J.-I. Jang, J.-C. Lee, *Met. Mater. Int.* 14 (2008) 9–13.
- [5] H.B. Ke, P. Wen, H.L. Peng, W.H. Wang, A.L. Greer, *Scr. Mater.* 64 (2011) 966–969.
- [6] B.-G. Yoo, K.-S. Kim, J.-H. Oh, U. Ramamurty, J.-I. Jang, *Scr. Mater.* 63 (2010) 1205–1208.
- [7] B.-G. Yoo, J.-H. Oh, Y.-J. Kim, K.-W. Park, J.-C. Lee, J.-I. Jang, *Intermetallics* 18 (2010) 1898–1901.
- [8] B.-G. Yoo, J.-Y. Kim, Y.-J. Kim, I.-C. Choi, S. Shim, T.Y. Tsui, H. Bei, U. Ramamurty, J.-I. Jang, *Int. J. Plasticity* 37 (2012) 108–118.
- [9] V. Keryvin, K. Eswar Prasad, Y. Gueguen, J.-C. Sangleboeuf, U. Ramamurty, *Philos. Mag.* 88 (2008) 1773–1790.
- [10] M.N.M. Patnaik, R. Narasimhan, U. Ramamurty, *Acta Mater.* 52 (2004) 3335–3345.
- [11] B.-G. Yoo, Y.-J. Kim, J.-H. Oh, U. Ramamurty, J.-I. Jang, *Scr. Mater.* 61 (2009) 951–954.
- [12] B.C. Wei, T.H. Zhang, W.H. Li, D.M. Xing, L.C. Zhang, Y.R. Wang, *Mater. Trans.* 46 (2005) 2959–2962.
- [13] A. Castellero, B. Moser, D.I. Uhlenhaut, F.H. Dalla Torre, J.F. Löffler, *Acta Mater.* 56 (2008) 3777–3785.
- [14] Y.J. Huang, Y.L. Chiu, J. Shen, J.J.J. Chen, J.F. Sun, *J. Mater. Res.* 24 (2009) 978–982.
- [15] Y.J. Huang, J. Shen, Y.L. Chiu, J.J.J. Chen, J.F. Sun, *Intermetallics* 17 (2009) 190–194.
- [16] J. Logan, M.F. Ashby, *Acta Metall.* 22 (1974) 1047–1054.
- [17] A.I. Taub, F. Spaepen, *J. Mater. Sci.* 16 (1981) 3087–3092.
- [18] K.-W. Park, J.-I. Jang, M. Wakeda, Y. Shibutani, J.-C. Lee, *Scr. Mater.* 57 (2007) 805–808.
- [19] I.-C. Choi, B.-G. Yoo, Y.-J. Kim, J.-I. Jang, *J. Mater. Res.* 27 (2012) 3–11.
- [20] A. Concustell, J. Sort, A.L. Greer, M.D. Baró, *Appl. Phys. Lett.* 88 (2006) 171911.
- [21] V. Ocelik, K. Csach, A. Kasardová, V.Z. Bengus, *Mater. Sci. Eng. A* 226–228 (1997) 851–855.
- [22] A.S. Argon, *Acta Metall.* 27 (1979) 47–58.
- [23] F. Spaepen, *Acta Metall.* 25 (1977) 407–415.
- [24] P. de Hey, J. Sietsma, A. Van Den Beukel, *Acta Mater.* 46 (1998) 5873–5882.
- [25] A. Concustell, J. Sort, G. Alcalá, S. Mato, J. Eckert, M.D. Baró, *J. Mater. Res.* 20 (2005) 2719–2725.